JOURNAL OF COMPUTATIONAL PHYSICS 121, 347–356 (1995)

A Variational Finite Element Method for Stationary Nonlinear Fluid–Solid Interaction

OMAR GHATTAS AND XIAOGANG LI

Computational Mechanics Laboratory, Department of Civil and Environmental Engineering, Carnegie Mellon University, Pittsburgh, Pennsylvania 15213

Received October 28, 1994

We consider the problem of the interaction of a stationary viscous fluid with an elastic solid that undergoes large displacement. The fluid is modeled by the stationary incompressible Navier–Stokes equations in an Eulerian frame of reference, while a Lagrangian reference frame and large displacement–small strain theory is used for the solid. A variational formulation of the problem is developed that ensures satisfaction of continuity of interface tractions and velocities. The variational formulation is approximated by a Galerkin finite element method, yielding a system of nonlinear algebraic equations in unknown fluid velocities and pressures and solid displacements. A Newton-like method is introduced for solution of the discrete system. The method employs a modified Jacobian that enables decomposition into separate fluid and solid subdomains. This domain decomposition avoids possible ill-conditioning of the Jacobian, as well as the need to compute and store geometric coupling terms between fluid and interface shape. The capability of the methodology is illustrated by solution of a problem of the flow-induced large displacements of an elastic infinite cylinder.

1. INTRODUCTION

Despite its importance, the problem of modeling the nonlinear interaction of a viscous fluid with a solid undergoing large deformation has remained a challenging problem in mechanics. Its resolution is of significant practical importance to such disciplines as aerospace, marine, automotive, and wind engineering. Such problems may arise, for instance, in the large-amplitude vibration of flexible aerodynamic components such as high aspect ratio wings and blades, in wind-induced deformation of towers, antennas, and lightweight bridges, in hydrodynamic flows around offshore structures, and in the interaction of biofluids with elastic vessels. The greatest difficulty here lies when two-way coupling occurs between fluid and solid: viscous flow produces tractions that deform the solid, while deformation of the solid influences the flow field and thus fluid tractions. Solid deformation influences the flow both by altering the fluid domain as well as by creating solid tractions that must be in equilibrium with the fluid tractions.

Because of its critical importance in aerospace applications, the problem of such nonlinear fluid–structure interaction has received considerable attention within the aerospace literature, where it is known as aeroelasticity. Classical approaches based on linear theory are well established [4, 9]. Certain nonlinear aeroelasticity phenomena have been amenable to analytical and semi-analytical study, and significant understanding of the physics of these problems has been elucidated in recent years [10]. Recently, interest has increased in *computational aeroelasticity*, i.e., in developing methods for direct numerical approximation of the governing nonlinear partial differential equations of the fluid–solid system [16–18, 3, 19, 11]. This interest has been motivated by advances in computational fluid dynamics and computational structural mechanics, and in the rapid growth in computational power.

The methods that have emerged within the past several years in the computational aeroelasticity literature employ different numerical approximations in fluid and solid domains, typically finite difference or volume methods for the fluid and finite elements for the solid. Fluid and solid are thus coupled *after* discretization. Since coupling is achieved after numerical approximation and approximations may not be consistent across the interface, continuity of interface tractions cannot be rigorously assured. In some approaches, fluid and solid are solved separately using existing numerical codes; thus coupling consists of a mechanism to transmit interface tractions between the two codes. Examples include [16–19]. Other approaches solve the coupled discrete equations simultaneously as a single set of nonlinear algebraic equations (in the context of steady problems) [11]. These methods have been criticized for resulting in possibly ill-conditioned Jacobian matrices of the coupled system, due to the disparity in solid and fluid behavior [19]. However, one ought to be able to apply various numerical linear algebraic devices to overcome this problem, as we shall do here. Nonlinear fluid–solid interaction problems have also been approximated by purely finite element methods, e.g., [8, 2, 1]. Coupling is again effected at the discrete level.

In this article, we address the stationary fluid–solid interaction problem. We target this problem because of its importance in optimal design, in which a design is optimized under steady-state conditions. In steady problems, if the solid deformation is so small that it does not change the fluid domain, the coupling is only one-way. In other words, we may solve the fluid equations, assuming a rigid solid, to obtain fluid tractions on the interface, and then to apply them to the solid to deform it. On the other hand, if the solid undergoes large deformation,

0021-9991/95 $12.00

coupling is two-way, even if the flow is steady; thus, we are not able to solve the fluid problem independently of the solid. This latter case is the subject of this article.

We are not aware of any variationally coupled numerical solutions of viscous fluid–finite elasticity interaction problems, a fact that motivates the present work. We develop a variational formulation that couples fluid and solid at the continuous level and thus assures continuity of interface tractions. We model the fluid by the stationary incompressible Navier–Stokes equations in an Eulerian frame of reference, while a Lagrangian reference frame and large displacement–small strain theory are used for the solid. Once coupled, we can systematically apply a numerical approximation—a Galerkin finite element method—to obtain a single set of nonlinear algebraic equations. We may then seek appropriate numerical methods for its solution, which may include linear algebraic devices such as domain decomposition to avoid ill-conditioning. The two main advantages of this method are that the variational formulation automatically ensures continuity of interface tractions, and it can be systematically translated into a unified finite element method for the coupled problem.

The rest of this paper is organized as follows. In Section 2, we develop the variational form of the viscous flow–finite elasticity interaction problem. A finite element approximation is constructed in Section 3, while Section 4 introduces a modified Newton method for solution of the resulting discrete system. The method is illustrated in Section 5 through the solution of a problem of flow-induced deformation of an infinite, elastic cylinder. We conclude with some remarks in Section 6.

2. VARIATIONAL FORMULATION

In this section we develop a variational formulation of the fluid–solid interaction problem in the context of a stationary, viscous, incompressible, Newtonian fluid, described by the Navier–Stokes equations, interacting with an isotropic piecewise-homogeneous elastic solid in a Lagrangian frame of reference. We assume that the solid is capable of large displacements, but that strains are small—a reasonable assumption for problems arising in aerospace, civil, and mechanical engineering.

The finite nature of solid displacements implies a geometric dependence of the flow field on the solid displacement. Consider a solid of finite extent surrounded by an infinite fluid, as depicted in Fig. 1. Define Ω_F as the fluid domain, Ω_S as the *undeformed* solid domain, Γ_F^1 as a boundary approximating the fluid far-field on which transactions are prescribed, Γ_F^2 as the portion of the far-field fluid boundary on which velocity is prescribed, Γ_S^1 as the undeformed solid boundary on which tractions are prescribed, Γ_S^2 as the undeformed solid boundary on which displacements are prescribed, Γ_{I_0} as the undeformed interface between solid and fluid, and Γ_I as the deformed interface between solid and fluid. The fluid field quantities are the pressure p, the velocity vector $\mathbf{v}$, the stress tensor $\boldsymbol{\sigma}_F$, and the rate of strain tensor $\mathbf{d}$. In the solid, the field quantities are the displacement vector $\mathbf{u}$, the Piola–Kirchhoff stress tensor $\mathbf{S}$, and the Green strain tensor $\mathbf{E}$. We shall have occasion to refer to the solid Eulerian stress tensor, which we denote $\boldsymbol{\sigma}_S$. Material constants are the fluid viscosity μ_F and density ρ, and the Lamé moduli of the solid, λ and μ_S. We take $\hat{\mathbf{v}}$ as the prescribed far-field fluid velocity, $\hat{\mathbf{t}}_F$ as the prescribed fluid traction, $\hat{\mathbf{u}}$ as the prescribed solid displacement, and $\hat{\mathbf{t}}_S$ as the prescribed solid traction. The fluid and solid body force are denoted $\mathbf{f}_F$ and $\mathbf{f}_S$. Define $\Gamma_F = \Gamma_F^1 \cup \Gamma_F^2$ and $\Gamma_S = \Gamma_S^1 \cup \Gamma_S^2$. We also define $\mathbf{n}$ as the unit outward normal to a deformed surface, $\mathbf{n}_0$ as the unit outward normal to an undeformed surface, $\mathbf{n}_{I_F}$ as the unit normal to the deformed fluid–solid interface, directed away from the fluid, and $\mathbf{n}_{I_S}$ as the unit normal to the deformed fluid–solid interface, directed away from the solid.

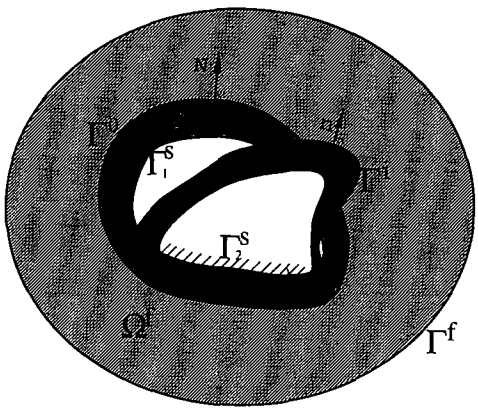

FIG. 1. Problem of fluid–solid interaction.

The conservation of momentum, conservation of mass, constitutive law, and strain rate–velocity equations of the fluid are

$$\rho_F(\mathbf{v}\cdot\nabla)\mathbf{v} - \operatorname{div}\boldsymbol{\sigma}_F = \mathbf{f}_F \quad \text{in } \Omega_F \tag{1}$$

$$\nabla\cdot\mathbf{v} = 0 \quad \text{in } \Omega_F \tag{2}$$

$$\boldsymbol{\sigma}_F = -p\mathbf{I} + 2\mu_F\mathbf{d} \quad \text{in } \Omega_F \tag{3}$$

$$\mathbf{d} = \tfrac{1}{2}(\nabla\mathbf{v} + \nabla\mathbf{v}^T) \quad \text{in } \Omega_F. \tag{4}$$

The constitutive law, equilibrium equations, and strain-displacement relations of the solid are given by

$$\mathbf{S} = \lambda\,\operatorname{tr}(\mathbf{E})\mathbf{I} + 2\mu_S\mathbf{E} \quad \text{in } \Omega_S \tag{5}$$

$$\operatorname{div}[(\mathbf{I} + \nabla\mathbf{u})\mathbf{S}] = \mathbf{f}_S \quad \text{in } \Omega_S \tag{6}$$

$$\mathbf{E} = \tfrac{1}{2}[\nabla\mathbf{u} + \nabla\mathbf{u}^T + \nabla\mathbf{u}\nabla\mathbf{u}^T] \quad \text{in } \Omega_S. \tag{7}$$

At the interface, coupling between fluid and solid requires that tractions and velocity be continuous:

$$\boldsymbol{\sigma}_S\mathbf{n}_{I_S} + \boldsymbol{\sigma}_F\mathbf{n}_{I_F} = \mathbf{0} \quad \text{on } \Gamma_I \tag{8}$$

$$\mathbf{v} = \dot{\mathbf{u}} = \mathbf{0} \quad \text{on } \Gamma_I. \tag{9}$$

Here, $\dot{\mathbf{u}}$ is the solid velocity, which is zero, according to the steady nature of the problem. Thus we have a no-slip condition on fluid velocity at the interface. Finally, the boundary conditions take the form

$$\boldsymbol{\sigma}_F \mathbf{n}_F = \hat{\mathbf{t}}_F \quad \text{on } \Gamma_F^1 \tag{10}$$

$$[(\mathbf{I} + \nabla\mathbf{u})\mathbf{S}]\,\mathbf{n}_0 = \hat{\mathbf{t}}_S \quad \text{on } \Gamma_S^1 \tag{11}$$

$$\mathbf{v} = \hat{\mathbf{v}} \quad \text{on } \Gamma_F^2 \tag{12}$$

$$\mathbf{u} = \hat{\mathbf{u}} \quad \text{on } \Gamma_S^2. \tag{13}$$

Here we have used the symbols div and ∇ to denote the spatial divergence and spatial gradient, respectively. See, for example, [15] for derivations of the governing equations of fluid and solid. Notice that the consequence of the small deformation assumption is to allow the use of Hooke's law for the solid constitutive relation (5).

We now proceed to establish the variational form of the problem. Let us assume, for simplicity of presentation, that the fluid and solid do not experience body forces and that the fluid and solid prescribed tractions are zero, i.e., $\mathbf{f}_F$, $\mathbf{f}_S$, $\mathbf{t}_F$, and $\hat{\mathbf{t}}_S$ are all zero. First, we substitute the strain rate–velocity relationship (4) into the fluid constitutive law (3), which is in turn substituted into the conservation of momentum equation (1). Then, multiplying the residual of the resulting equation by the test function $\mathbf{w}$, integrating over the fluid domain, and applying Green's formula, we obtain the weak form of the conservation of momentum equation,

$$a(\mathbf{v}, \mathbf{w}) + b(p, \mathbf{w}) + c(\mathbf{v}, \mathbf{v}, \mathbf{w}) = \int_{\Gamma_I} \mathbf{w} \cdot \boldsymbol{\sigma}_F \mathbf{n}\, d\Gamma_I(\mathbf{u}) + \int_{\Gamma_F} \mathbf{w} \cdot \boldsymbol{\sigma}_F \mathbf{n}\, d\Gamma_F(\mathbf{u}), \tag{14}$$

where

$$a(\mathbf{v}, \mathbf{w}) = \int_{\Omega_F} \frac{\mu_F}{2} (\nabla\mathbf{v} + \nabla\mathbf{v}^{\mathrm{T}}) : (\nabla\mathbf{w} + \nabla\mathbf{w}^{\mathrm{T}})\, d\Omega_F(\mathbf{u}) \tag{15}$$

$$b(p, \mathbf{w}) = -\int_{\Omega_F} p \nabla \cdot \mathbf{w}\, d\Omega_F(\mathbf{u}) \tag{16}$$

$$c(\mathbf{v}, \mathbf{v}, \mathbf{w}) = \int_{\Omega_F} \rho \mathbf{w} \cdot (\mathbf{v} \cdot \nabla)\mathbf{v}\, d\Omega_F(\mathbf{u}) \tag{17}$$

and where the symbol : denotes the scalar product of two tensors. Since we wish to consider problems in which the displacement of solid may be large enough to influence the flow, we indicate the dependence of the fluid domain on the solid displacement in the definition of the domains of integration of the bilinear functionals $a(\cdot, \cdot)$ and $b(\cdot, \cdot)$ and the trilinear functional $c(\cdot, \cdot, \cdot)$. The second term on the right side of (14) can be rewritten as

$$\int_{\Gamma_F} \mathbf{w} \cdot \boldsymbol{\sigma}_F \mathbf{n}\, d\Gamma_F(\mathbf{u}) = \int_{\Gamma_F^1} \mathbf{w} \cdot \boldsymbol{\sigma}_F \mathbf{n}\, d\Gamma_F^1(\mathbf{u}) + \int_{\Gamma_F^2} \mathbf{w} \cdot \boldsymbol{\sigma}_F \mathbf{n}\, d\Gamma_F^2(\mathbf{u}). \tag{18}$$

We shall require that the test function $\mathbf{w}$ satisfy the homogeneous essential boundary condition $\mathbf{v} = \mathbf{0}$ on Γ_F^2, implying that the second term on the right of (18) is zero. Furthermore, since $\hat{\mathbf{t}}_F$ is zero, and in light of (10) the first term on the right side of (18) vanishes. Therefore,

$$\int_{\Gamma_F} \mathbf{w} \cdot \boldsymbol{\sigma}_F \mathbf{n}\, d\Gamma_F(\mathbf{u}) = 0. \tag{19}$$

Next, we write the conservation of mass equation in weak form by multiplying (2) by the test function q and integrating over the domain of the fluid:

$$\int_{\Omega_F} q \nabla \cdot \mathbf{v}\, d\Omega_F(\mathbf{u}) = -b(q, \mathbf{v}) = 0. \tag{20}$$

Again, note the dependence of the fluid domain, and thus the weak form, on the solid displacement.

The weak form of the solid equilibrium equation is established by first substituting the expression for the Green's strain tensor (7) into the constitutive law (5) and then substituting the resulting expression for the Piola–Kirchhoff stress into the equilibrium equation. Multiplying the residual of the resulting equation by the test function $\mathbf{r}$, integrating over the domain, and applying Green's formula, we obtain the weak form of the displacement form of the equilibrium equations,

$$\int_{\Omega_S} \nabla\mathbf{r} : [(\mathbf{I} + \nabla\mathbf{u})\,\mathbf{S}(\mathbf{u})]\, d\Omega_S = \int_{\Gamma_{I_0}} \mathbf{r} \cdot [(\mathbf{I} + \nabla\mathbf{u})\,\mathbf{S}(\mathbf{u})]\,\mathbf{n}_0\, d\Gamma_{I_0} + \int_{\Gamma_S} \mathbf{r} \cdot [(\mathbf{I} + \nabla\mathbf{u})\,\mathbf{S}(\mathbf{u})]\,\mathbf{n}_0\, d\Gamma_S, \tag{21}$$

where the relationship between Piola–Kirchhoff stress and displacement is given by

$$\mathbf{S}(\mathbf{u}) = \tfrac{1}{2}\lambda\, \mathrm{tr}[\nabla\mathbf{u} + \nabla\mathbf{u}^{\mathrm{T}} + \nabla\mathbf{u}\nabla\mathbf{u}^{\mathrm{T}}]\,\mathbf{I} + \mu_S[\nabla\mathbf{u} + \nabla\mathbf{u}^{\mathrm{T}} + \nabla\mathbf{u}\nabla\mathbf{u}^{\mathrm{T}}]. \tag{22}$$

Notice that, since we are in a Lagrangian frame of reference, the unit normal is with respect to the *undeformed* geometry, and the interface is between fluid and undeformed solid, denoted Γ_{I_0}. The solid boundary Γ_S consists of the portion on which displacements are specified, Γ_S^2, and the portion on which tractions are specified, Γ_S^1. Thus, the second term on the right of (21) can be rewritten as

$$\begin{aligned}\int_{\Gamma_S} \mathbf{r} \cdot [(\mathbf{I} + \nabla \mathbf{u})\, \mathbf{S}(\mathbf{u})]\, \mathbf{n}_0\, d\Gamma_S \\ = \int_{\Gamma_S^1} \mathbf{r} \cdot [(\mathbf{I} + \nabla \mathbf{u})\, \mathbf{S}(\mathbf{u})]\, \mathbf{n}_0\, d\Gamma_S^1 \\ + \int_{\Gamma_S^2} \mathbf{r} \cdot [(\mathbf{I} + \nabla \mathbf{u})\, \mathbf{S}(\mathbf{u})]\, \mathbf{n}_0\, d\Gamma_S^2.\end{aligned} \tag{23}$$

Since $\hat{\mathbf{t}}_S$ is zero, and in light of (11), the first term on the right of this equation is zero. Furthermore, we shall require that the test function $\mathbf{r}$ satisfy the homogeneous essential boundary condition $\mathbf{u} = \mathbf{0}$ on Γ_S^2. Therefore, the second term vanishes over Γ_S^2. Thus,

$$\int_{\Gamma_S} \mathbf{r} \cdot [(\mathbf{I} + \nabla \mathbf{u})\, \mathbf{S}(\mathbf{u})]\, \mathbf{n}_0\, d\Gamma_S = \mathbf{0}. \tag{24}$$

The first term on the right of (21) can be transformed to the deformed geometry by noting that $(\mathbf{I} + \nabla \mathbf{u})\, \mathbf{S} = \mathbf{T}$, the Lagrangian stress tensor. The surface traction expressed in terms of the Lagrangian stress at a point $\mathbf{s}'$ on the undeformed interface is identical to the surface traction expressed in terms of the Eulerian stress at its image $\mathbf{s}''$ on the deformed interface. Thus, we may write

$$\mathbf{T}(\mathbf{s}')\, \mathbf{n}_0(\mathbf{s}') = \boldsymbol{\sigma}_S(\mathbf{s}'')\, \mathbf{n}(\mathbf{s}''). \tag{25}$$

Therefore, provided

$$\mathbf{r}(\mathbf{s}') = \mathbf{w}(\mathbf{s}''), \tag{26}$$

i.e. the restriction of the test functions $\mathbf{r}$ to the undeformed interface is equal to the restriction of $\mathbf{w}$ to the deformed interface, the first term on the right side of (21) can be rewritten as

$$\int_{\Gamma_{I_0}} \mathbf{r} \cdot [(\mathbf{I} + \nabla \mathbf{u})\, \mathbf{S}(\mathbf{u})]\, \mathbf{n}_0\, d\Gamma_{I_0} = \int_{\Gamma_I} \mathbf{w} \cdot \boldsymbol{\sigma}_S \mathbf{n}\, d\Gamma_I. \tag{27}$$

To simplify the left side of (21), we separate $\mathbf{S}$ into $\mathbf{S}^L$, a tensor that depends linearly on displacement, and $\mathbf{S}^N$, one whose dependence is nonlinear, in fact, quadratic,

$$\mathbf{S}^L = \lambda\, \mathrm{tr}(\nabla \mathbf{u})\mathbf{I} + \mu_S(\nabla \mathbf{u} + \nabla \mathbf{u}^{\mathrm{T}}) \tag{28}$$

$$\mathbf{S}^N = \tfrac{1}{2}\lambda\, \mathrm{tr}(\nabla \mathbf{u} \nabla \mathbf{u}^{\mathrm{T}})\, \mathbf{I} + \mu_S(\nabla \mathbf{u} \nabla \mathbf{u}^{\mathrm{T}}) \tag{29}$$

so that (22) can be rewritten as $\mathbf{S} = \mathbf{S}^L + \mathbf{S}^N$. Thus, the domain integral on the left side of (21) can be rewritten as the sum of terms that depend linearly, quadratically, and cubically on the derivatives of $\mathbf{u}$,

$$\begin{aligned}\int_{\Omega_S} \nabla \mathbf{r} : [(\mathbf{I} + \nabla \mathbf{u})\, \mathbf{S}(\mathbf{u})]\, d\Omega_S = d(\mathbf{u}, \mathbf{r}) + e(\mathbf{u}, \mathbf{u}, \mathbf{r}) \\ + f(\mathbf{u}, \mathbf{u}, \mathbf{u}, \mathbf{r}),\end{aligned} \tag{30}$$

where

$$d(\mathbf{u}, \mathbf{r}) = \int_{\Omega_S} \nabla \mathbf{r} : \mathbf{S}^L(\mathbf{u})\, d\Omega_S \tag{31}$$

$$e(\mathbf{u}, \mathbf{u}, \mathbf{r}) = \int_{\Omega_S} \nabla \mathbf{r} : [\mathbf{S}^N(\mathbf{u}) + \nabla \mathbf{u}\, \mathbf{S}^L(\mathbf{u})]\, d\Omega_S \tag{32}$$

$$f(\mathbf{u}, \mathbf{u}, \mathbf{u}, \mathbf{r}) = \int_{\Omega_S} \nabla \mathbf{r} : [\nabla \mathbf{u}\, \mathbf{S}^N(\mathbf{u})]\, d\Omega_S. \tag{33}$$

The condition of continuity of interface tractions can now be imposed. Adding Eqs. (14) and (21) and making use of (19), (24), and (27), gives

$$\begin{aligned}a(\mathbf{v}, \mathbf{w}) + b(p, \mathbf{w}) + c(\mathbf{v}, \mathbf{v}, \mathbf{w}) + d(\mathbf{u}, \mathbf{r}) + e(\mathbf{u}, \mathbf{u}, \mathbf{r}) \\ + f(\mathbf{u}, \mathbf{u}, \mathbf{u}, \mathbf{r}) = \int_{\Gamma_I} \mathbf{w} \cdot (\boldsymbol{\sigma}_F \cdot \mathbf{n}_{I_F} + \boldsymbol{\sigma}_S \cdot \mathbf{n}_{I_S})\, d\Gamma_I(\mathbf{u}).\end{aligned} \tag{34}$$

The right side of this equation is just zero, in view of the continuity of traction condition (8).

We are in a position now to state the unified variational form of the viscous flow-finite elasticity interaction problem:

Find $\mathbf{v} \in \mathbf{H}_0^1(\Omega)$, $p \in L^2(\Omega)$, and $\mathbf{u} \in \mathbf{H}_0^1(\Omega)$ such that

$$\begin{aligned}&a(\mathbf{v}, \mathbf{w}) + b(p, \mathbf{w}) + c(\mathbf{v}, \mathbf{v}, \mathbf{w}) + d(\mathbf{u}, \mathbf{r}) \\ &\quad + e(\mathbf{u}, \mathbf{u}, \mathbf{r}) + f(\mathbf{u}, \mathbf{u}, \mathbf{u}, \mathbf{r}) = 0 \\ &\quad \text{for all } \mathbf{w} \in \mathbf{H}_0^1(\Omega_F),\ \mathbf{r} \in \mathbf{H}_0^1(\Omega_S) \\ &b(q, \mathbf{v}) = 0 \quad \text{for all } q \in L^2(\Omega_F),\end{aligned} \tag{35}$$

where the functionals $a(\cdot, \cdot)$, $b(\cdot, \cdot)$, $c(\cdot, \cdot, \cdot)$, $d(\cdot, \cdot)$, $e(\cdot, \cdot, \cdot)$, and $f(\cdot, \cdot, \cdot, \cdot)$ are defined by expressions (15), (16), (17), (31), (32), and (33), respectively. Here, $\mathbf{H}_0^1(\Omega_F)$ is the Sobolev subspace of all functions having one square integrable derivative over Ω_F and that vanish on Γ_F^2 and outside of Ω_F, $L^2(\Omega_F)$ is the space of functions that are square integrable over Ω_F and that vanish outside of Ω_F, and $\mathbf{H}_0^1(\Omega_S)$ is the Sobolev subspace of all functions having one square integrable derivative over Ω_S and that vanish on Γ_S^2 and outside of Ω_S. The essential boundary conditions $\mathbf{v} = \hat{\mathbf{v}}$ and $\mathbf{u} = \hat{\mathbf{u}}$ must be enforced on Γ_F^2 and Γ_S^2, respectively, as must the no-slip condition $\mathbf{v} = \mathbf{0}$ on Γ_I.

3. FINITE ELEMENT APPROXIMATION

Let us define the finite element approximations $\mathbf{v}_h$, p_h, and $\mathbf{u}_h$,

$$\mathbf{v}_h = \sum_{i=1}^{n^v} \boldsymbol{\phi}_i(\mathbf{x}) v_i \tag{36}$$

$$p_h = \sum_{j=1}^{n^p} \chi_j(\mathbf{x}) p_j \tag{37}$$

$$\mathbf{u}_h = \sum_{k=1}^{n^u} \boldsymbol{\psi}_k(\mathbf{x}) u_k, \tag{38}$$

where v_i, p_j, and u_k are approximations of velocity, pressure, and displacement at nodes i, j, and k, respectively. The basis function families $\boldsymbol{\phi}_i$, χ_j, and $\boldsymbol{\psi}_k$ define finite element spaces $\mathcal{V}_h$, $\mathcal{P}_h$, and $\mathcal{U}_h$ for velocity, pressure, and displacement, respectively:

$$\mathcal{V}_h = \text{span}\{\boldsymbol{\phi}_1, ..., \boldsymbol{\phi}_{n^v}\} \tag{39}$$

$$\mathcal{P}_h = \text{span}\{\chi_1, ..., \chi_{n^p}\} \tag{40}$$

$$\mathcal{U}_h = \text{span}\{\boldsymbol{\psi}_1, ..., \boldsymbol{\psi}_{n^u}\}. \tag{41}$$

Let $\mathcal{V}_h \subset \mathbf{H}_0^1(\Omega_F)$, $\mathcal{P}_h \subset L^2(\Omega_F)$, and $\mathcal{U}_h \subset \mathbf{H}_0^1(\Omega_S)$; i.e., the finite element spaces $\mathcal{V}_h$, $\mathcal{P}_h$, and $\mathcal{U}_h$ are subspaces of the infinite dimensional spaces in (35). In order to satisfy condition (26), we require that fluid velocity and solid displacement shape functions be identical, when restricted to the interface between solid and fluid. An example of this is given by combining quadratic triangles in the solid with the Taylor–Hood element in the fluid. The Taylor–Hood element employs a quadratic approximation of velocity in conjunction with a linear approximation of pressure; thus, solid displacement and fluid velocity shape functions are identical on the interface.

Applying the Galerkin method to the problem (35) yields the discrete problem:

Find $\mathbf{v}_h \in \mathcal{V}_h$, $p_h \in \mathcal{P}_h$, and $\mathbf{u}_h \in \mathcal{U}_h$ such that

$$\begin{aligned} &a(\mathbf{v}_h, \mathbf{w}_h) + b(p_h, \mathbf{w}_h) + c(\mathbf{v}_h, \mathbf{v}_h, \mathbf{w}_h) + d(\mathbf{u}_h, \mathbf{r}_h) \\ &\quad + e(\mathbf{u}_h, \mathbf{u}_h, \mathbf{r}_h) + f(\mathbf{u}_h, \mathbf{u}_h, \mathbf{u}_h, \mathbf{r}_h) = 0 \\ &\quad \text{for all } \mathbf{w}_h \in \mathcal{V}_h, \mathbf{r}_h \in \mathcal{U}_h, \end{aligned} \tag{42}$$

and

$$b(q, \mathbf{v}_h) = 0 \quad \text{for all } q \in \mathcal{P}_h.$$

The discrete problem (42) is a system of nonlinear algebraic equations. To show the explicit form of these equations, let us first distinguish between nodes lying in the interior and those on the interface. Let

$$\begin{aligned} n^v &= n_F^v + n_I^v \\ n^p &= n_F^p + n_I^p \\ n_s &= n_S^s + n_I^s, \end{aligned} \tag{43}$$

where the subscript F indicates the number of nodes belonging strictly to the fluid domain, S the number of nodes belonging strictly to the solid domain, and I the number of nodes belonging to the interface. So, for example, the n^v velocity nodes are composed of n_F^v fluid domain nodes as well as n_I^v interface nodes. Notice that the satisfaction of condition (26) implies that the number of velocity and displacement interface nodes are equal. Let us call this number n_I:

$$n_I \equiv n_F^v = n_S^u. \tag{44}$$

Let the fluid velocity nodes be ordered such that nodes 1, ..., n_I lie on the interface and $n_I + 1$, ..., n^v lie in the fluid domain as well as that portion of the fluid boundary on which tractions are prescribed. Similarly, the solid displacement nodes are ordered such that nodes 1, ..., n_I lie on the interface and $n_I + 1$, ..., n^u lie in the solid domain as well as that portion of the solid boundary on which tractions are prescribed.

We are able now to elucidate the structure of the discrete problem (42). In the fluid, we have the n_F^v discrete conservation of momentum equations

$$\begin{aligned} &\sum_{i=1}^{n^v} a(\boldsymbol{\phi}_i, \boldsymbol{\phi}_l) v_i + \sum_{j=1}^{n^p} b(\chi_j, \boldsymbol{\phi}_l) p_j \\ &\qquad + \sum_{i,r=1}^{n^v} c(\boldsymbol{\phi}_i, \boldsymbol{\phi}_r, \boldsymbol{\phi}_l) v_i v_r = 0, \\ &\qquad l = n_I + 1, ..., n^v, \end{aligned} \tag{45}$$

and the n_F^p discrete conservation of mass equations

$$\sum_{i=1}^{n^v} b(\chi_m, \boldsymbol{\phi}_i) v_i = 0, \quad m = n_I^p + 1, ..., n^p. \tag{46}$$

In the solid, the n_S^u discrete equilibrium equations are given by

$$\begin{aligned} &\sum_{k=1}^{n^u} d(\boldsymbol{\psi}_k, \boldsymbol{\psi}_n) u_k + \sum_{k,s=1}^{n^u} e(\boldsymbol{\psi}_k, \boldsymbol{\psi}_s, \boldsymbol{\psi}_n) u_k u_s \\ &\qquad + \sum_{k,s,t=1}^{n^u} f(\boldsymbol{\psi}_k, \boldsymbol{\psi}_s, \boldsymbol{\psi}_t, \boldsymbol{\psi}_n) u_k u_s u_t = 0, \\ &\qquad n = n_I + 1, ..., n^u. \end{aligned} \tag{47}$$

Finally, on the interface, we have the n_I discrete traction continuity equations,

$$\sum_{i=1}^{n^v} a(\boldsymbol{\phi}_i, \boldsymbol{\phi}_y)v_i + \sum_{j=1}^{n^p} b(\chi_j, \boldsymbol{\phi}_y)p_j + \sum_{i,r=1}^{n^v} c(\boldsymbol{\phi}_i, \boldsymbol{\phi}_r, \boldsymbol{\phi}_y)v_i v_r + \sum_{k=1}^{n^u} d(\boldsymbol{\psi}_k, \boldsymbol{\psi}_y)u_k + \sum_{k,s=1}^{n^u} e(\boldsymbol{\psi}_k, \boldsymbol{\psi}_s, \boldsymbol{\psi}_y)u_k u_s + \sum_{k,s,t=1}^{n^u} f(\boldsymbol{\psi}_k, \boldsymbol{\psi}_s, \boldsymbol{\psi}_t, \boldsymbol{\psi}_y)u_k u_s u_t = 0, \quad y = 1, \ldots, n_I, \tag{48}$$

and the n_I^p discrete conservation of mass equations,

$$\sum_{i=1}^{n^v} b(\chi_z, \boldsymbol{\phi}_i)v_i = 0, \quad z = 1, \ldots, n_I^p. \tag{49}$$

Let us define vectors of unknown nodal quantities: let $\mathbf{v}_F \in \Re^{n_F^v}$ represent the fluid nodal velocities, $\mathbf{p}_F \in \Re^{n_F^p}$ the fluid pressures, $\mathbf{v}_I \in \Re^{n_I}$ the interface velocities, $\mathbf{p}_I \in \Re^{n_I^p}$ the interface pressures, $\mathbf{u}_S \in \Re^{n_S^u}$ the solid displacements, and $\mathbf{u}_I \in \Re^{n_I}$ the interface displacements. We can rewrite the discrete equations (45)–(49) symbolically as

$$\begin{aligned} \mathbf{h}_F^v(\mathbf{v}_F, \mathbf{p}_F, \mathbf{v}_I, \mathbf{p}_I, \mathbf{u}_I) &= \mathbf{0} \\ \mathbf{h}_F^p(\mathbf{v}_F, \mathbf{v}_I, \mathbf{u}_I) &= \mathbf{0} \\ \mathbf{h}_S^u(\mathbf{u}_S, \mathbf{u}_I) &= \mathbf{0} \\ \mathbf{h}_I(\mathbf{v}_F, \mathbf{p}_F, \mathbf{v}_I, \mathbf{p}_I, \mathbf{u}_S, \mathbf{u}_I) &= \mathbf{0} \\ \mathbf{h}_I^p(\mathbf{v}_F, \mathbf{v}_I, \mathbf{u}_I) &= \mathbf{0}, \end{aligned} \tag{50}$$

where $\mathbf{h}_F^v \in \Re^{n_F^v}$ represents conservation of momentum in the fluid, $\mathbf{h}_F^p \in \Re^{n_F^p}$ conservation of mass in the fluid, $\mathbf{h}_S^u \in \Re^{n_S^u}$ equilibrium in the solid, $\mathbf{h}_I \in \Re^{n_I}$ continuity of interface tractions, and $\mathbf{h}_I^p \in \Re^{n_I^p}$ conservation of mass on the interface. It appears that we have $n^v + n^p + n^u - n_I$ equations in $n^v + n^p + n^u$ unknowns. However, the continuity of interface velocity condition (9) implies that $\mathbf{v}_I = \mathbf{0}$, and we are thus left with an equal number of equations and unknowns upon enforcing this condition in (50).

Note that, in addition to $\mathbf{h}_S^u$, the fluid and interface residuals $\mathbf{h}_F^v$, $\mathbf{h}_F^p$, $\mathbf{h}_I^p$, and $\mathbf{h}_I$ depend on the interface displacements $\mathbf{u}_I$. This is implied in the domain of integration of the functionals $a(\cdot, \cdot)$ (15), $b(\cdot, \cdot)$ (16), and $c(\cdot, \cdot, \cdot)$ (17), i.e., in the dependence of the flow on the interface geometry.

4. SOLUTION OF THE DISCRETE SYSTEM

We discuss in this section a Newton-like method for solving the system of nonlinear algebraic equations (50). Our discussion will be kept brief; a more extensive discussion of this and other solution methods for finite element approximations of viscous flow-finite elasticity interaction will be presented in the future [12].

Let us first begin by rewriting (50) as

$$\begin{aligned} \mathbf{h}_F(\mathbf{x}_F, \mathbf{x}_I) &= 0 \\ \mathbf{h}_S(\mathbf{x}_S, \mathbf{x}_I) &= 0 \\ \mathbf{h}_I(\mathbf{x}_F, \mathbf{x}_S, \mathbf{x}_I) &= 0, \end{aligned} \tag{51}$$

where

$$\mathbf{h}_F = \begin{Bmatrix} \mathbf{h}_F^v \\ \mathbf{h}_F^p \\ \mathbf{h}_I^p \end{Bmatrix}, \quad \mathbf{x}_F = \begin{Bmatrix} \mathbf{v}_F \\ \mathbf{p}_F \\ \mathbf{p}_I \end{Bmatrix}, \quad \mathbf{x}_S = \mathbf{u}_S, \quad \mathbf{x}_I = \mathbf{u}_I. \tag{52}$$

Note that the fluid equations $\mathbf{h}_F = \mathbf{0}$ include the equations for conservation of mass on the interface, $\mathbf{h}_I^p = \mathbf{0}$, and the fluid variables $\mathbf{x}_F$ include the interface pressures $\mathbf{p}_I$. Accordingly, the interface variables consist only of the interface displacements. The reason for this choice of partitioning will become apparent.

Newton's method for the nonlinear system $\mathbf{h}(\mathbf{x}) = \mathbf{0}$ consists of iterating on solution of the linear system

$$\mathbf{J}(\mathbf{x}^k)(\mathbf{x}^{k+1} - \mathbf{x}^k) = -\mathbf{h}(\mathbf{x}^k) \tag{53}$$

until convergence, given an initial iterate $\mathbf{x}^0$. Here, $\mathbf{J}$ is the Jacobian of $\mathbf{h}$ with respect to $\mathbf{x}$. A Newton step for the discrete system (51) takes the form

$$\begin{bmatrix} \mathbf{J}_{FF}^k & \mathbf{0} & \mathbf{J}_{FI}^k \\ \mathbf{0} & \mathbf{J}_{SS}^k & \mathbf{J}_{SI}^k \\ \mathbf{J}_{IF}^k & \mathbf{J}_{IS}^k & \mathbf{J}_{II_F}^k + \mathbf{J}_{II_S}^k \end{bmatrix} \begin{Bmatrix} \Delta\mathbf{x}_F \\ \Delta\mathbf{x}_S \\ \Delta\mathbf{x}_I \end{Bmatrix} = -\begin{Bmatrix} \mathbf{h}_F^k \\ \mathbf{h}_S^k \\ \mathbf{h}_I^k \end{Bmatrix}, \tag{54}$$

where

$$\Delta\mathbf{x} = \mathbf{x}^{k+1} - \mathbf{x}^k. \tag{55}$$

Here, the superscript k indicates evaluation of the residual $\mathbf{h}$ and the Jacobian $\mathbf{J}$ at the point $\mathbf{x}^k$, and the interface–interface coupling matrix $\mathbf{J}_{II}$ includes contributions from both solid and fluid:

$$\mathbf{J}_{II} = \mathbf{J}_{II_F} + \mathbf{J}_{II_S} \tag{56}$$

The Newton iteration (54) entails two difficulties. First, the Jacobian matrix, because of the disparity between fluid and solid behavior, can be very ill-conditioned. Second, the coupling terms between fluid and interface variables in general render the matrices $\mathbf{J}_{FI}$ and $\mathbf{J}_{II_F}$ dense. The density of these matrices is a consequence of the dependence of the domains of integration of $a(\cdot, \cdot)$, $b(\cdot, \cdot)$, and $c(\cdot, \cdot, \cdot)$ on the interface displacements. In the case of $\mathbf{J}_{FI}$, all fluid nodal velocities and

pressures may be coupled to all interface nodal displacements, since a change in any interface displacement potentially moves the fluid mesh everywhere. The matrix $\mathbf{J}_{II_F}$ derives its density from the fact that the interface traction continuity equation (48) includes contributions from the first layer of fluid elements, which change with a movement in the interface. Thus, the potential exists for coupling between all interface variables. $\mathbf{J}_{II_S}$ contains nonzeroes contributed by the solid terms in (48), i.e., the terms involving $d(\cdot, \cdot)$, $e(\cdot, \cdot, \cdot)$, and $f(\cdot, \cdot, \cdot)$. These are just the standard solid stiffness matrix coupling terms, so the coupling is local in nature.

The exact sparsity pattern depends on the moving mesh scheme employed, but, in general, the storage requirements and arithmetic complexity associated with $\mathbf{J}_{FI}$ and $\mathbf{J}_{II_F}$ can be quite severe. Therefore, we consider an *approximate* Newton's method obtained by ignoring the fluid–interface coupling matrix $\mathbf{J}_{FI}$ and the contribution of the fluid to the interface–interface coupling matrix, $\mathbf{J}_{II_F}$. The resulting Jacobian in (54) becomes block-lower triangular. Thus, the fluid variables can be found by solving the linear system

$$\mathbf{J}_{FF}^k \Delta \mathbf{x}_F = -\mathbf{h}_F^k \tag{57}$$

for $\Delta \mathbf{x}_F$. The change in the displacements (both interior and interface) can then be found by solving

$$\begin{bmatrix} \mathbf{J}_{SS}^k & \mathbf{J}_{SI}^k \\ \mathbf{J}_{IS}^k & \mathbf{J}_{II_S}^k \end{bmatrix} \begin{Bmatrix} \Delta \mathbf{x}_S \\ \Delta \mathbf{x}_I \end{Bmatrix} = - \begin{Bmatrix} \mathbf{h}_S^k \\ \mathbf{h}_I^k + \mathbf{J}_{IF}^k \Delta \mathbf{x}_F \end{Bmatrix}. \tag{58}$$

This method avoids the ill-conditioning associated with the coupled problem by employing a "domain decomposition" into separate fluid and solid subdomains. Large storage requirements associated with geometric coupling matrices are avoided by ignoring these terms while constructing the Jacobian. However, since the residual in (54) is calculated correctly, we are guaranteed that, if the method converges, it must converge to the correct solution. This can be seen from (53): the only way that $\Delta \mathbf{x}$ can be zero is for $\mathbf{h}$ to be zero, provided only that $\mathbf{J}$ is nonsingular, regardless of whether or not it represents the true Jacobian. The price we pay for this approximate Jacobian is that we must give up the Newton guarantee of local quadratic convergence.

We now establish that the modified Jacobian is indeed nonsingular. First, the fluid step (57) can be seen to be just a Newton step for the Navier–Stokes equations, with a rigid boundary given by the current deformed interface, and a no-slip boundary condition imposed on the interface. Thus, the linear system (57) has a unique solution (provided, of course, that we are away from singular bifurcation or turning points). Second, the solid step (58) can also be regarded as a Newton step for the solid equilibrium equations. The term $\mathbf{J}_{IF}^k \Delta \mathbf{x}_F$ is the incremental "loading" that the linearized fluid induces on the solid interface. So this linear step too must have a unique solution (provided again we are away from buckling points). Thus, the solution of (54) is unique, and the approximate Jacobian is nonsingular.

We stress that this decoupling is a numerical device designed to remedy the twin problems of ill-conditioning and storage and arithmetic complexity. The residual equations $\mathbf{h} = \mathbf{0}$ still contain the correct variational coupling between fluid and solid, and the solution reflects that—only the convergence rate to the solution is affected.

5. EXAMPLE: FLOW-INDUCED DEFORMATION OF AN INFINITE ELASTIC CYLINDER

We have built a code that implements the finite element approximation of Section 3 in two dimensions and solves the resulting nonlinear algebraic system using the method of Newton form described in Section 4. We employ a simple continuation strategy to help globalize the solution. Our code discretizes both solid and fluid with triangular elements and uses quadratic shape functions for velocity and displacement and linear shape functions to approximate pressure. The Taylor–Hood element pair is known to satisfy the Ladyzhenskaya–Babuska–Brezzi stability condition, e.g., [5], and the complimentary choice of quadratic triangles for the solid ensures the satisfaction of the interface compatibility condition (26). The Taylor–Hood element produces L_2 norm errors of order h^3 for velocity and h^2 for pressure [14], while quadratic triangles for elasticity problems produce L_2 norm errors of order h^3 for displacements [6] (provided in both cases the solution is sufficiently smooth). The linear solves (57) and (58) are performed using the unsymmetric multifrontal sparse LU factorization code UMFPACK [7].

As the solid deformations change from one iteration to the next, the movement of the fluid mesh is computed by the so-called elastic analogy, a common technique in the aeroelasticity literature. The fluid domain is treated as an elastic solid, and the move in the location of the interface is expressed through imposed displacements. Solution of this elastic analogy yields the change in location of fluid nodes. This technique was apparently first used in [1].

In order to illustrate our methodology, we next present results of a physical problem solved by our code. The problem is viscous flow about an infinite elastic cylinder, and is depicted in Fig. 2. The problem thus is two-dimensional. The cylinder is of diameter d and thickness t and is composed of material having elastic modulus E and Poisson ratio ν. The fluid is characterized by density ρ and viscosity μ. The computational domain extends a distance of $6d$ upstream of the cylinder, $18d$ downstream, and $12d$ above and below its center. Flow is from left to right with a free-stream horizontal velocity of U and no vertical velocity. Boundary conditions downstream of the cylinder are that the flowfield is traction-free. On the top and bottom boundaries are imposed zero vertical flow and zero horizontal traction. Both vertical and horizontal components of

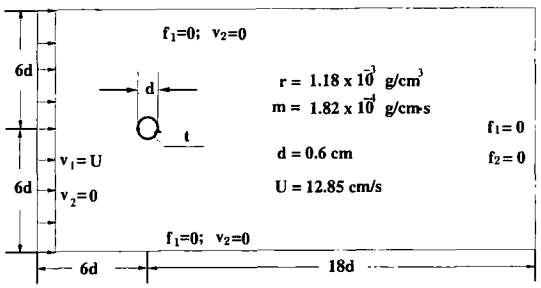

FIG. 2. Stationary flow passing an elastic circular cylinder.

displacement are fixed at nodes along the horizontal axis of symmetry at the downstream end of the cylinder. Nodes lying on the upstream end of the horizontal axis of symmetry are prevented from moving vertically but are free to translate horizontally. The inner boundary of the cylinder is traction-free. Two cases are solved: one for which the cylinder is nearly rigid and one for which the cylinder is quite flexible.

Values of ρ, μ, d, and U used in the computation are given in the figure. These correspond to a Reynolds number of about 50, which is kept low to prevent the formation of the Kármán vortex street. A Poisson ratio of 0.3 is taken for the solid. The undeformed mesh is shown in Fig. 3. Although it cannot be seen in the figure, two quadratic elements are used through the thickness of the cylinder.

Data describing the mesh are given in Table I. A convergence criterion of $\|\mathbf{h}\| \leq 10^{-6}$ is used to terminate the Newton iteration at each continuation step.

Figure 4 shows streamlines corresponding to the converged flowfield in the vicinity of the cylinder for the case of the nearly rigid cylinder ($E = 10000$, $t = 0.06$). Figure 5 shows a close-up of the velocity field for this case. The resulting displacement of the cylinder is negligible and does not affect the flow field. Two standing eddies of moderate size, symmetric about the horizontal axis, are observed behind the cylinder, as expected for flow around a rigid cylinder in this regime.

Figure 6 shows the resulting displacement and a portion of the flow field when the cylinder is more flexible ($E = 1000$, $t = 0.02$) and thus undergoes large displacement. A close-up view of the velocity field for this case is depicted in Fig. 7. The undeformed shape of the cylinder is shown in addition to the deformed shape. The flow field depicted corresponds to the converged solution, i.e., to the deformed shape. The standing eddies extend more than twice as far downstream as in the rigid case, due to the much more bluff shape assumed by the deformed cylinder.

In the latter case of the elastic cylinder, convergence is obtained in a total of 38 iterations by a simple continuation scheme, first increasing the Reynolds number to the desired value, then decreasing the solid stiffness. The iteration history for the case of the elastic cylinder is shown in Fig. 8.

The abscissa represents cumulative Newton (linear) steps. The ordinate represents the value of the residual for the given values of Reynolds number and solid stiffness. As the figure shows, the appropriate nonlinear parameter is advanced when the residual falls below the convergence tolerance, always using the converged field quantities corresponding to the previous parameter to initiate the approximate Newton method. The

TABLE I

Mesh Data

Item	Number
Solid nodes	416
Fluid nodes	3552
Interface nodes	104
Boundary nodes	152
Total nodes	4224
Solid elements	208
Fluid elements	1840
Total elements	2048
Velocity unknowns	7166
Pressure unknowns	984
Displacement unknowns	824
Interface unknowns	205
Total unknowns	9179

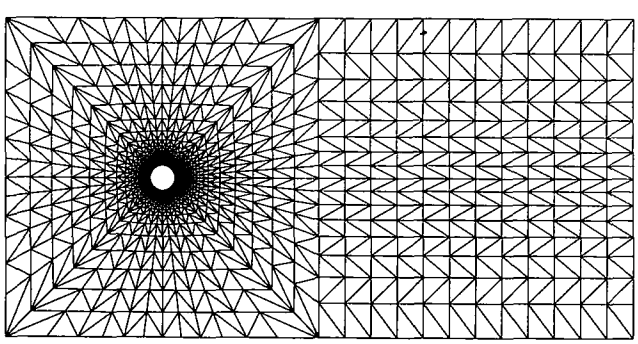

FIG. 3. Finite element mesh.

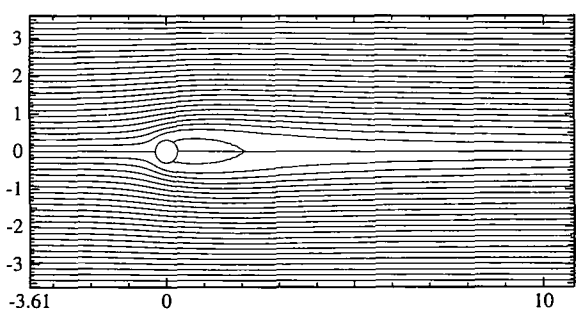

FIG. 4. Streamlines about a nearly rigid cylinder.

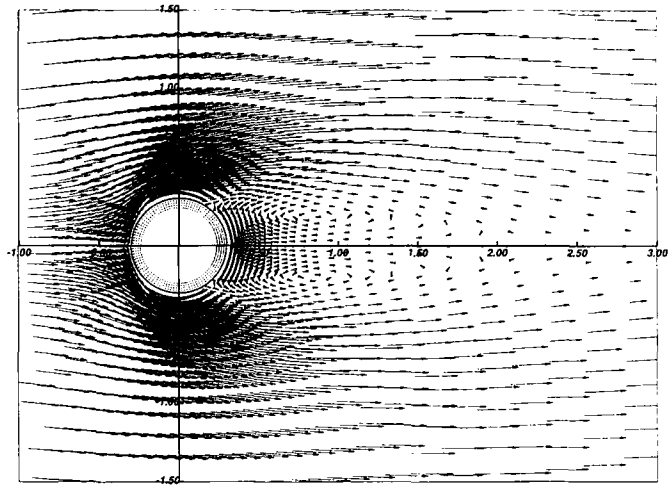

FIG. 5. Close-up view of the velocity field corresponding to the nearly rigid cylinder.

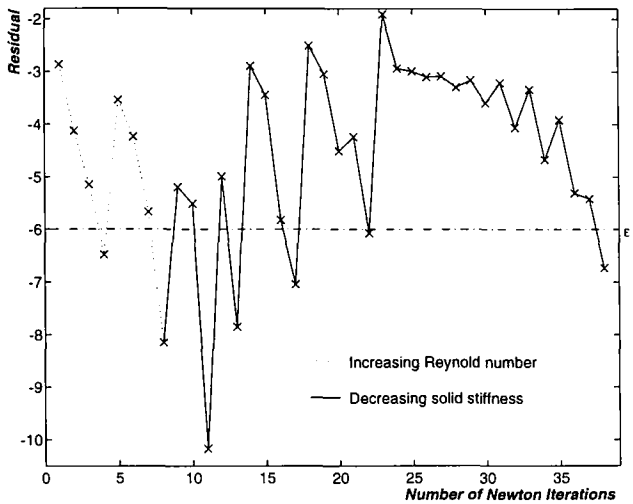

FIG. 8. Iteration history showing continuation steps and cumulative Newton iterations.

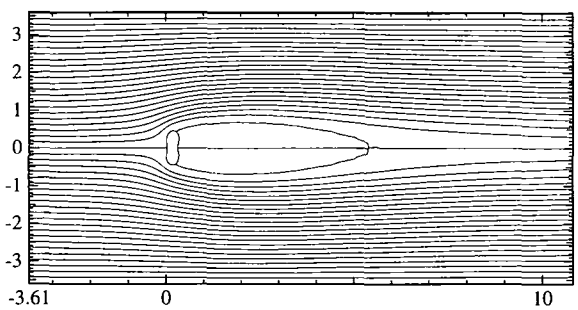

FIG. 6. Streamlines about an elastic cylinder.

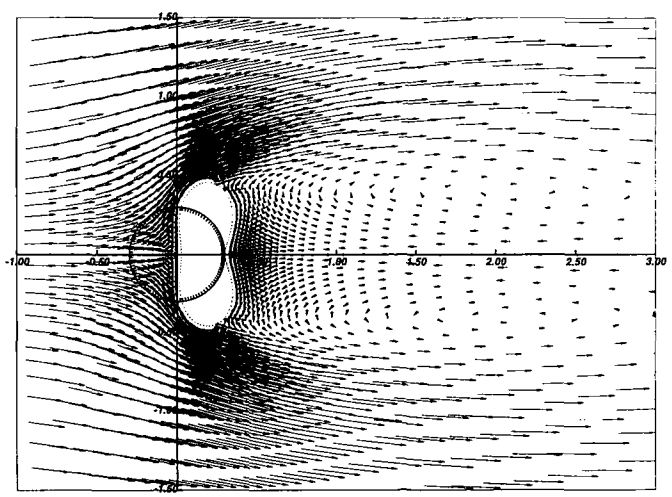

FIG. 7. Close-up view of the velocity field corresponding to the elastic cylinder.

dotted line indicates increasing Reynolds number, while the solid line represents decreasing solid stiffness. Although the convergence scheme is conservative, it is quite effective, and we have been able to solve a number of flow-induced large displacement problems using it.

6. CONCLUDING REMARKS

We have developed a methodology for numerical approximation of the interaction of a stationary viscous fluid with a elastic solid that undergoes large displacement. The fluid is modeled with respect to an Eulerian frame of reference by the stationary incompressible Navier–Stokes equations, while a Lagrangian reference frame and large displacement–small deformation theory is used for the solid. A variational formulation of the problem is developed that ensures satisfaction of continuity of interface tractions and velocities. The variational formulation is approximated by a Galerkin finite element method, yielding a system of nonlinear algebraic equations is unknown fluid velocities and pressures and solid displacements. A Newton-like method is introduced for solution of the discrete system. The method employs a modified Jacobian that enables decomposition into separate fluid and solid subdomains. This domain decomposition avoids possible ill-conditioning of the Jacobian, as well as the need to compute and store geometric coupling terms between fluid and interface shape. The method is illustrated by solution of a problem of the flow-induced large deformation of an elastic cylinder.

Work is underway to extend the methodology to unsteady problems. In another thrust, we have developed methods for sensitivity analysis of the models described here [13]. Together, these methods should prove useful for solving problems in multidisciplinary design optimization.

ACKNOWLEDGMENTS

We thank Jacobo Bielak and Earl Dowell for their comments and suggestions, as well as those of an anonymous referee. This research was partially supported by Algor, Inc., and by the Engineering Design Research Center, an NSF Engineering Research Center at Carnegie-Mellon University. In addition, the work of the first author was supported by NSF Grant DDM-9114678. This work was conducted on computers purchased with funds provided in part by NSF Equipment Grant BCS-9212819.

REFERENCES

1. J. Argyris, J. St. Doltsinis, H. Fischer, and H. Wüstenberg, *Comput. Methods Appl. Mech. Eng.* **51,** 289 (1985).
2. T. Belytschko, D. P. Flanagan, and J. M. Kennedy, *Comput. Methods Appl. Mech. Eng.* **33,** 669 (1982).
3. O. O. Bendiksen, "A New Approach to Computational Aeroelasticity," in *32nd Structures, Structural Dynamics, and Materials Conference,* p. 1712 (AIAA, Washington, DC, 1991).
4. R. L. Bisplinghoff and H. Ashley, *Principles of Aeroelasticity* (Wiley, New York, 1962).
5. J. Boland and R. Nicolaides, *SIAM J. Numer. Anal.* **20,** 722 (1983).
6. P. Ciarlet, *The Finite Element Method for Elliptic Problems* (North-Holland, Amsterdam, 1978).
7. T. A. Davis and I. S. Duff, Technical Report TR-93-018, CIS Dept., University of Florida, Gainesville, FL, 1993 (unpublished).
8. J. Donea, S. Giuliani, and J. P. Halleux, *Comput. Methods Appl. Mech. Eng.* **33,** 689 (1982).
9. E. H. Dowell, H. C. Curtiss, R. H. Scanlan, and F. Sisto, *A Modern Course in Aeroelasticity* (Sijthoff & Noordhoff, The Netherlands, 1980).
10. E. H. Dowell and M. Ilgamov, *Studies in Nonlinear Aeroelasticity* (Springer Verlag, New York/Berlin, 1988).
11. F. F. Felker, *AIAA J.* **31**(1), 148 (1993).
12. O. Ghattas and X. Li, working manuscript.
13. O. Ghattas and X. Li, AIAA Paper 94-4399 (unpublished).
14. M. Gunzburger, *Finite Element Methods for Viscous Incompressible Flows* (Academic Press, New York, 1989).
15. M. E. Gurtin, *Introduction to Continuum Mechanics* (Academic Press, New York, 1981).
16. G. P. Guruswamy, *AIAA J.* **28**(3), 461 (1990).
17. G. P. Guruswamy, *AIAA J.* **28**(12), 2077 (1990).
18. G. P. Guruswamy, "Vortical Flow Computations on a Flexible Blended Wing–Body Configuration," in *32nd Structures, Structural Dynamics, and Materials Conference* (AIAA, Washington, DC, 1991), p. 719.
19. G. P. Guruswamy, "Coupled Finite-Difference/Finite Element Approach for Wing–Body Aeroelasticity," in *Fourth AIAA/USAF/NASA/OAI Symposium on Multidisciplinary Analysis and Optimization, 1992,*" p. 1.